All-Atom Numerical Studies of Self-Assembly of Zwitterionic Peptide Amphiphiles

Stefan Tsonchev,* Alessandro Troisi, George C. Schatz, and Mark A. Ratner

Department of Chemistry and Center for Nanofabrication and Molecular Self-Assembly, Northwestern University, Evanston, Illinois 60208

Received: May 17, 2004; In Final Form: July 2, 2004

We present an approach to study the self-assembly of organic macromolecules, based on all-atom empirical force field calculations. The approach is applied to self-assemblies of zwitterionic peptide amphiphiles possessing large dipoles in their hydrophilic headgroups. The assembly is built from the bottom up by first optimizing the diad amphiphile, which is then used as a basic unit to subsequently first build quartets, and then 4×4 supercells of molecules to be studied in periodic boundary conditions. Explicit water solvent is added to the surface of the periodic structures and molecular dynamics simulations are performed on them. The calculations reveal an interesting structure of the resulting assemblies: the dipoles in the upper parts of the headgroups are aligned in an antiparallel fashion with respect to each other and along one of the periodic axes, while hydrogen bonds in the lower, rigid parts of the headgroups form a parallel beta sheet along the same direction. It is shown that the structure exhibits the tendency to curve around an axis parallel to the direction of the dipoles and the hydrogen bonds, forming a cylindrical micelle.

1. Introduction

Rapid developments in the field of nanotechnology have opened the door to the creation of large number of new materials expected to find applications in a wide variety of fields, ranging from new medical treatments to the electronics industry.[1−6] A common feature of these new substances is that they are all built through self-assembly of macromolecules or particles of nanoscale size and their properties are predetermined by the molecular characteristics of their constituent elements.

The potential impact of these materials in all aspects of modern society has in turn generated interest in the scientific community to study them and the possibilities for their synthesis. Experimentalists have achieved great success in this regard,[7,8] and theoretical studies have been initiated aimed at understanding of the mechanisms of self-assembly and how to design and control the properties of the resulting material through an appropriate selection of the initial conditions and the structure and chemical properties of the precursor molecules.[9,10]

Recently, we studied an interesting class of such self-assembling peptide amphiphiles,[11−13] which were created by Stupp and co-workers,[14−17] and were intended for use in medical treatments as artificial bone substitutes and as templates for neuron regeneration. The self-assembling macromolecule studied by us is shown in Figure 1. It possesses a hydrophobic tail and a hydrophilic headgroup consisting of two major parts: a rigid, lower region and a flexible, upper part exposed to the solution. In an earlier work we concluded that at the appropriate pH, as done in the experiment,[14] large dipoles appear in the headgroups, which, together with the anticipated hydrogen bonds, play an important role in the shape and stability of these self-assembled nanostructures.[12] The goal of our study was not only to understand the stability and structure of the resulting self-assemblies, but also to develop methods to study other similar systems and make the connection between the characteristics of the starting macromolecules and the initial conditions on one side, and the properties of the final assembly on the other. First, we developed a model to predict the shape and structure of the final assemblies, which is based on reducing the complex macromolecules to simpler structures retaining their overall shape, symmetry, and charges.[12] Later, we performed all-atom molecular dynamics (MD) simulations on the self-assemblies to find their detailed structure, as well as their stability, and the role of dipole−dipole interactions and hydrogen-bonding in it.[13] In these simulations, we used implicit solvent to screen the interactions between the hydrophilic headgroups.

This work presents detailed description of the procedure used to build and optimize the self-assembly, given in Section 2. The assembly is then optimized in periodic boundary conditions (PBC), discussed in Section 3, and studied with MD simulations using explicit water solvent, which is described in Section 4. Our approach to investigate the stability of the assembly as a function of its curvature around each of the periodic axes is discussed in Section 5, leading to the conclusion that a cylindrical assembly would be the most stable one. In Section 6 we conclude and discuss possible implications of this study and the potential applications of the approach presented in this paper.

2. Building the Self-Assembly

A rigorous numerical study at the atomistic level of a self-assembly process such as the one studied here is beyond the capability of modern computers. The time scale of such processes is on the order of seconds, to minutes and hours, while an MD simulation on a system of this size would be possible up to times on the order of nanoseconds. Monte Carlo simulations are also out of the question due to the large parameter space needed to be explored to find the (global) energy minimum of the self-assembled nanostructure. Therefore, we will use an approach to self-assembly that does not possess the rigor of the standard methods mentioned above; however, it is statistically rigorous and does follow a procedure resembling what we believe is the real process of self-assembly. We will assume that binary collisions between the macromolecules in solution,

* E-mail: stefan@chem.northwestern.edu.

10.1021/jp047880e CCC: $27.50
Published on Web 09/08/2004

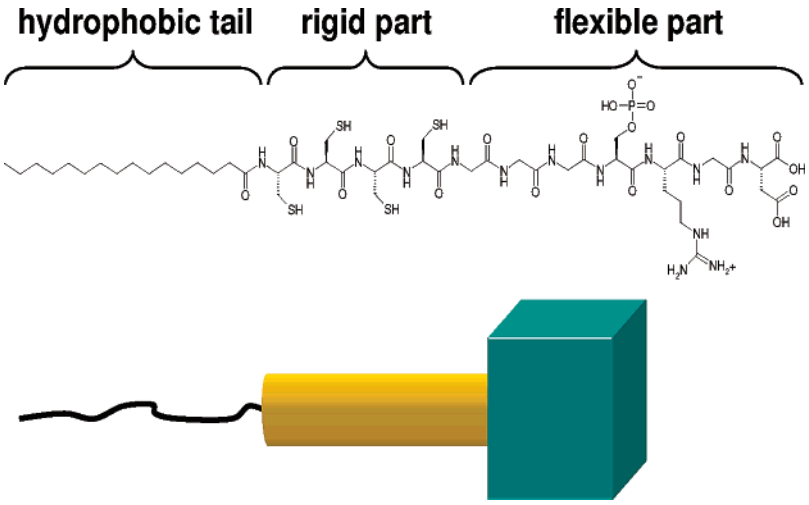

Figure 1. Self-assembling peptide amphiphile studied in this work with a corresponding cartoon of the main parts of the molecule.

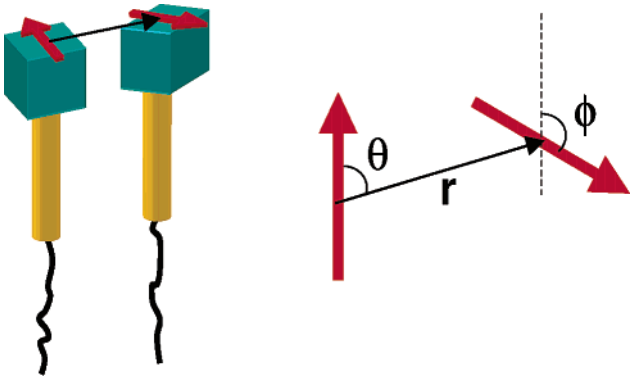

Figure 2. Scheme of the initial conditions for the optimization of the diad amphiphile. We vary the distance between the two dipoles, *r*, as well as their relative orientation, defined by the angles θ and ϕ.

being most frequent, would start the self-assembly from a diad amphiphile kernel (a dimer of amphiphiles). Hence, in our approach the diad amphiphile is the major building block from which the complete nanostructure will be built.

The MM3 force field,[18] as implemented in the *Tinker* package[19] was used in this paper for the optimization, the simulated annealing, and the MD. Hydrogen atoms were constrained at their ideal bond distance using the *rattle* algorithm.[20] MD simulations were run within the canonical ensemble using the Berendsen algorithm.[21]

Starting from two unoptimized macromolecules, we optimize their diad by statistically sampling the initial conditions to find its global energy minimum. Let us define the *z* coordinate of the system as extending along the length of one of the molecules. Optimizing the diads starting from a number of initial conditions in which the two molecules are displaced with respect to each other along *z*, shows that the most stable diads are those which have the same *z* coordinates for both molecules, that is, the molecules tend to maximize their interactions along their length. Therefore, we will not vary the initial configurations with respect to *z* and will keep the two molecules parallel, but will vary the initial conditions in a plane perpendicular to *z*. In Figure 2 we show a scheme of the initial conditions to be varied. We have projected the dipoles of the molecules on a plane perpendicular to *z*, and will vary the distance between the centers of these projections, *r*, and their relative orientation defined by the angles θ and ϕ (see Figure 2). We will sample distances *r* from 3.5 to 7.0 Å, at every 0.5 Å, while the angles θ and ϕ will be sampled at every 30°. Thus, we minimize, and then perform simulated annealing on the diad starting from more than a thousand different initial configurations, after which we compare the stability of the resulting structures. This comparison is shown in Figure 3, where we plot the energy of the system as a function of the angles θ and ϕ. It is seen that with respect to the angle θ, the distribution of stable structures is wide and centered roughly around 90°. That is, the two molecules prefer to have a "sideways" position with respect to each other, while with respect to the angle ϕ the stable structures are localized between angles of 150° and 180°. In other words, their dipoles prefer to have an antiparallel orientation with respect to each other, as is to be expected. After the optimization, we have calculated the energy of several of the most stable diads without the charges of their dipoles but keeping their structure as is, and have found less than half of the energy plotted in Figure 3, which includes the interactions of the bare charges in the headgroups. This indicates that the electrostatic interactions between the large dipoles of the molecules are a dominant factor in the self-assembly process, and that our strategy of sampling the initial configurations based on the dipoles' orientation is appropriate.

We select the most stable diad amphiphile, shown in Figure 4, and use it as a building block for the entire structure. In Figure 4 we also show a top view of the diad structure, emphasizing the dipoles' antiparallel orientation, and a simplified schematic representation of the diad, containing only the dipoles, with a black parallelogram at its lower left end to indicate the low symmetry of the structure, which must be taken into account when statistically sampling the possible initial configurations in the following steps of building the self-assembly.

Next, we group two diads together into quartets of molecules to be optimized and annealed by analogous statistical sampling of the initial conditions. The sampling procedure for the quartets is schematically summarized in Figure 5, where two examples of the initial conditions for the optimization of the quartets are shown. In Figure 5, the *z* coordinate is perpendicular to the plane of view, and we vary the distance between the diads along the *x* and *y* coordinates. We also rotate the diads with respect to each other at every 90°. Thus, we start from several hundred initial configurations for the quartets, which are minimized and annealed, and the most stable resulting structures are selected for further building of the self-assembly. We find seven quartets substantially more stable than the rest, by more than 20 kcal/mol. They belong to six groups; the most stable quartet of each group is shown in Figure 6, with the corresponding schematic diagram above it. These quartets, named *A*, *B*, *C*, *D*, *E*, *F*, and

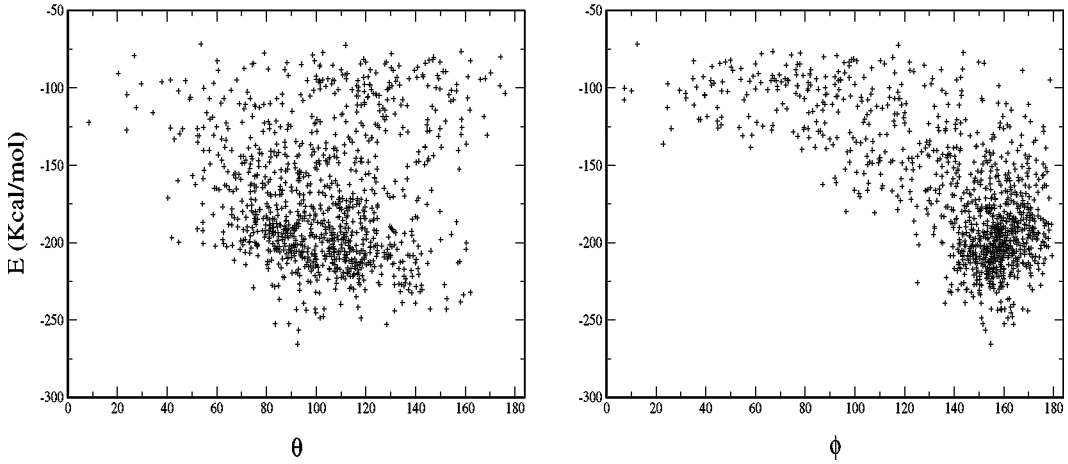

Figure 3. Energy of the minimized diad as a function of the angles θ and ϕ, defined in Figure 2.

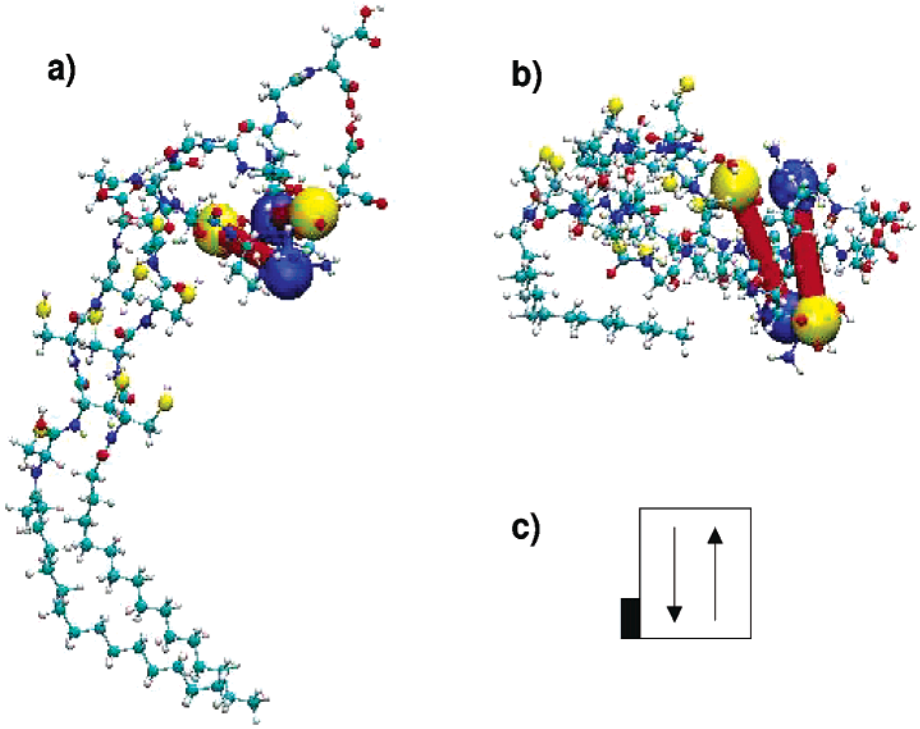

Figure 4. Optimized diad amphiphile used as a basic unit to build the entire self-assembly is shown in (a), where the dipoles in the hydrophilic headgroups are shown with the positive (negative) charges represented by blue (yellow) spheres. A top view of the diad is shown in (b), with its corresponding schematic diagram given in (c). The black parallelogram at the lower left end of the diagram emphasizes the low symmetry of the structure.

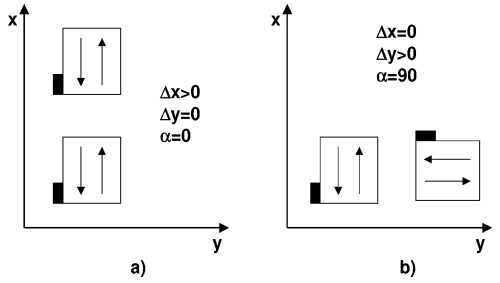

Figure 5. Sampling scheme for the initial quartet configurations. In the example of (a) the second diad is displaced with respect to the first one along *x*, without being rotated, while in (b) the second diad is displaced along *y* and is rotated by an angle $\alpha = 90°$.

G, are used to build supercells of 4 × 4 blocks of 16 amphiphiles, which are to be minimized and annealed with periodic boundary conditions (PBC). Since there are more intermolecular interactions in the PBC calculations than in the elementary cells alone, the stability order of the quartets after minimization and annealing in PBC may change, and that is why we have selected the most stable quartets of several kinds, to make sure that we have the most stable possible structure at the end. The schematic diagrams of the supercells of 16 amphiphiles are shown in Figure 7, with structures *E* and *F* represented by the same diagram.

3. Periodic Boundary Conditions Analysis

We have used the *xtalmin* routine of *tinker*[19] to simultaneously optimize the periodic lengths and structure of each of the seven elementary cells. First, the periodic lengths of each structure are optimized with *xtalmin* without any solvent, and later on implicit solvent is added according to the methods of Eisenberg and McLachlan (asp),[22] Sheraga et al. (sasa),[23] and Truhlar et al. (hct).[24] A comparison of the stability of the resulting structures is shown in Table 1.

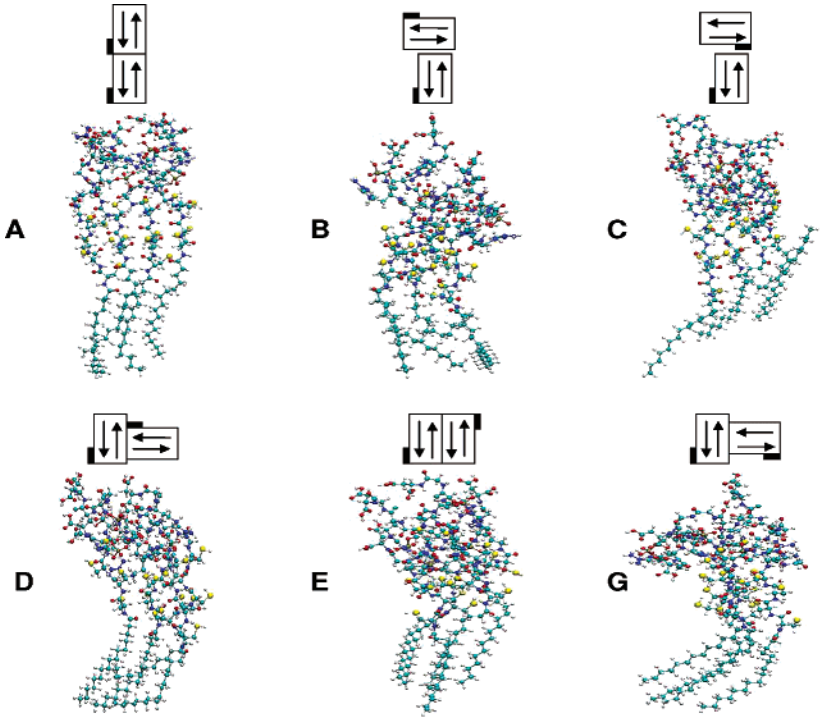

Figure 6. Six of the selected most stable quartets, with the corresponding schematic diagram above each structure.

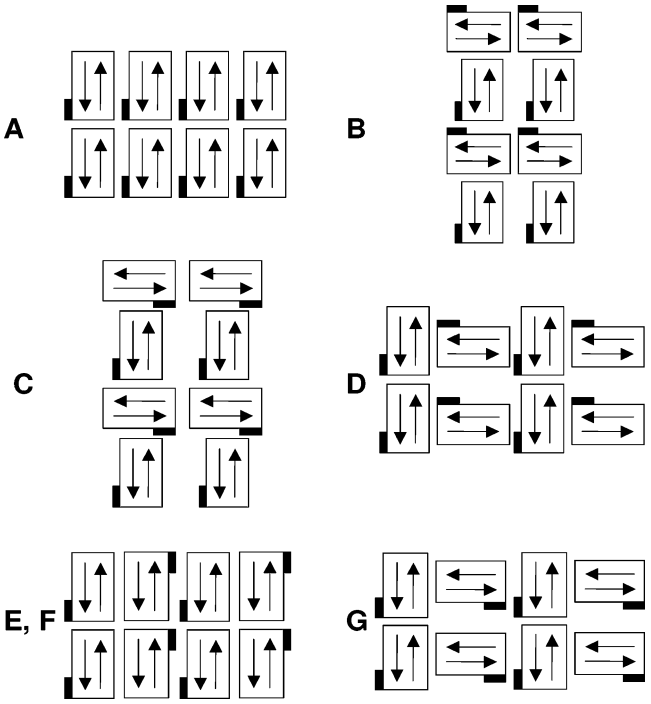

Figure 7. Schematic diagrams of the 4 × 4 supercells studied in PBC.

Structure A is clearly the most stable. It possesses the lowest energy of all, regardless of the method of calculation used. It also has the smallest area of the elementary cell, and is, therefore, the densest structure, which correlates very well with its stability. This conclusion is expected based on the scheme of Figure 7, from which it is clear that we can attribute the stability of structure *A* to the order of the dipole orientations, allowing close packing and long-range attractive interactions.

4. Molecular Dynamics Simulations with Explicit Solvent

We performed MD simulations on structure *A* with explicit water solvent. First, we added more than 450 water molecules above the surface of the assembly, enough to form at least three layers, to ensure the proper screening of the charges. Then, we first minimized, and subsequently annealed, the whole system with periodic boundary conditions. After more than one hundred annealings, the most stable configuration obtained in this way was chosen as a starting point for dynamic simulation. The system was first equilibrated for 20 ps, after which the simulation was run for 0.5 ns. Snapshots were taken at every picosecond. In Figure 8 we show a sample of the structure. From analysis of the snapshots we conclude that the dipoles on the surface of the structure are oriented in an antiparallel fashion along one of the periodic directions, *x*, while the hydrogen bonds between the lower rigid parts of the headgroups form an effective parallel beta-sheet oriented in the same direction, analogous to the results we obtained earlier with implicit water solvent.[13] We have found approximately 2.66 hydrogen bonds per molecule in the beta-sheet. There are also hydrogen bonds between the upper, flexible parts of the headgroups crosslinking the molecules in random directions. In addition, most of the thiol groups in the cysteine residues of the beta-sheet, which can be covalently bound to polymerize the assembly, are oriented in a direction approximately perpendicular to that of the dipoles and hydrogen bonds. A plot of the dipoles on the surface of the elementary cell, replicated three times along *x*, is shown in Figure 9. Most dipoles form antiparallel doublets,

TABLE 1: Comparison between the Total Energies (in kcal/mol) of the Seven Periodic Structures[a]

structure	no solvent	asp	sasa	hct	area[b]
A	−2438.16	−2964.98	−3268.15	−3275.10	743.93
B	−2285.22	−2736.58	−2834.25	−2889.96	847.80
C	−2299.85	−2752.72	−2908.75	−3118.08	976.16
D	−2307.20	−2739.24	−2852.28	−2926.85	1040.58
E	−2311.02	−2790.84	−2899.83	−2906.67	1085.11
F	−2260.97	−2697.56	−2802.77	−3253.16	1132.22
G	−2205.77	−2727.91	−2797.74	−2952.71	989.33

[a] It should be noted that the absolute values of the energies have no meaning outside of the purpose of the comparison. [b] The elementary cell area is shown in Å^2.

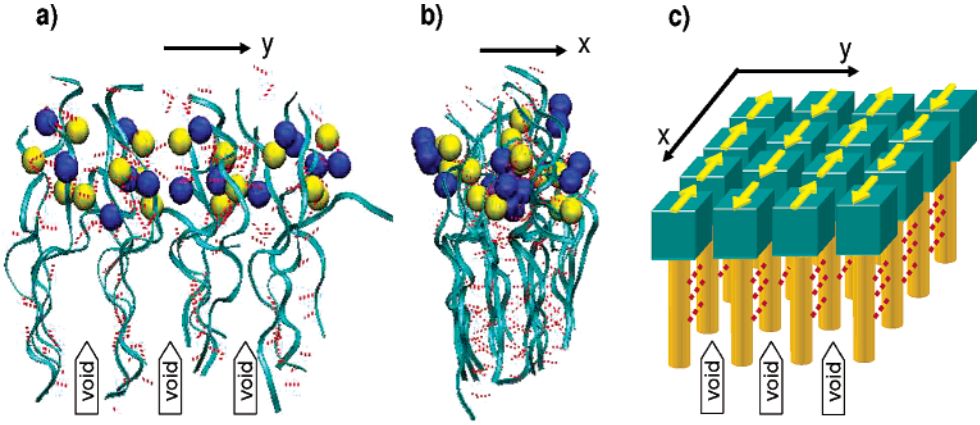

Figure 8. Optimized structure from the viewpoints of the two axes, *y* and *x*, shown in (a) and (b), respectively, where the positive (negative) charges of the dipoles in the headgroups are represented by blue (yellow) spheres, and the hydrogen bonds are represented by dotted red lines. The backbones of the molecules are represented by ribbons, and the tails, as well as the water molecules, are omitted.[25] It is seen that the density along *x* is higher, while the voids along *y* indicate the tendency of the structure to curve in that direction. A schematic representation of the elementary cell of the periodic structure is shown in part (c), with the yellow arrows in the upper parts of the headgroups representing the dipoles.

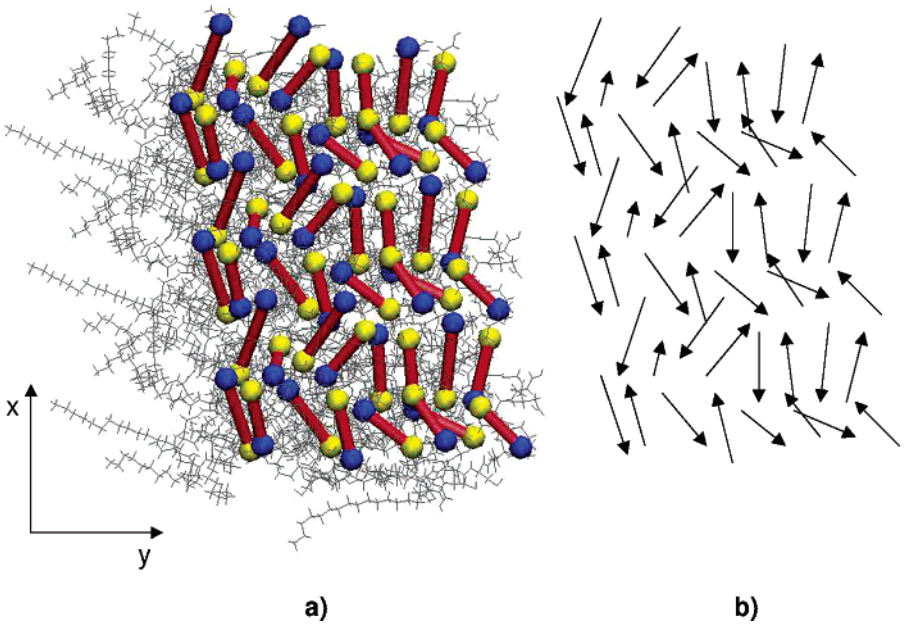

Figure 9. Top-view snapshot of the dipolar positions on the micellar surface (a), with an extraction of the dipolar vectors shown in (b), where antiparallel pairs of dipoles, roughly oriented along the *x* periodic direction, are clearly distinguishable.

roughly aligned with the *x* direction, with some exceptions, as is to be expected from a dynamic system at finite temperature. In Figure 10 we show a histogram of the distribution of angles between each dipole and the *x* axis, as well as the distribution of the same angles for the hydrogen bonds between the rigid parts of the hydrophilic headgroups. The approximately bimodal distributions of these angles illustrates the antiparallel dipole orientation, as well as the formation of a parallel beta sheet, both oriented along this axis.[26] However, a comparison with our earlier study[13] shows that with explicit water solvent this effect is less pronounced, as can be seen from the lower peaks of the histogram in Figure 10 compared to Figure 3 in Tsonchev et al.[13] Hence, including explicit water solvent leads to stronger screening of the electrostatic interactions in the headgroups, compared to the implicit solvent models[22−24] used by us earlier. We have attributed this difference to the "soaking" of the hydrophilic headgroups by the water solvent, observed by us during the annealing and equilibration stage of the simulations, when water molecules from the solvent penetrate deep into the headgroups and form hydrogen bonds with the peptides. This effect is obviously difficult to capture by the implicit solvent models. It should also be noted that the dipoles' motion is restricted to a narrow range around their equilibrium positions and the structure is very stable on the time scale of the simulation.

5. Optimization of the Curvature of the Self-Assembly

An examination of snapshots from the MD simulations of structure *A*, such as the one shown in Figure 8, shows voids along the *y* periodic direction. This indicates that the planar periodic structure may not be the most stable one and it would probably have the tendency to curve around the *x* axis. To determine this tendency, the approach briefly introduced by us earlier is used,[13] the details of which are as follows. We introduce curvature on the structure according to the scheme of Figure 11, where the *z* axis is perpendicular to the surface of the structure, and the length of the structure along the direction *y* is *a*. The origin of the Cartesian coordinates is on the curvature axis, while the center of the cell is at $(Y, Z) = (0, Z^0)$. Curvature around the *x* axis is introduced by an isomorphism that maps the rectangular cross-section of the elementary cell in the *y*, *z*

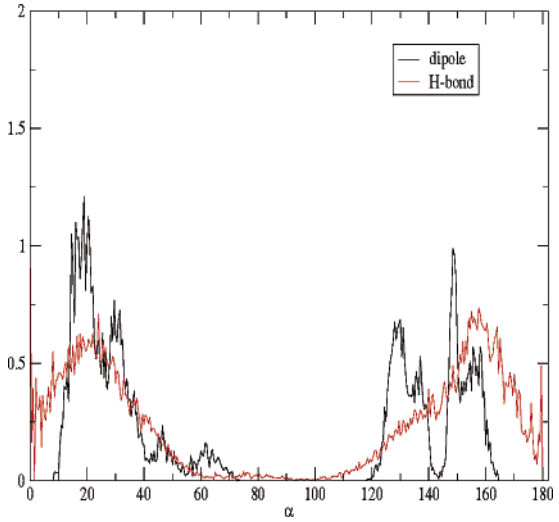

Figure 10. Distributions of angles α between the dipoles or hydrogen bonds between the lower, rigid parts of the headgroups and the *x* axis of the assembly. The antiparallel orientation of the dipoles and hydrogen bonds along this axis is evident from the approximately bimodal character of the distributions.

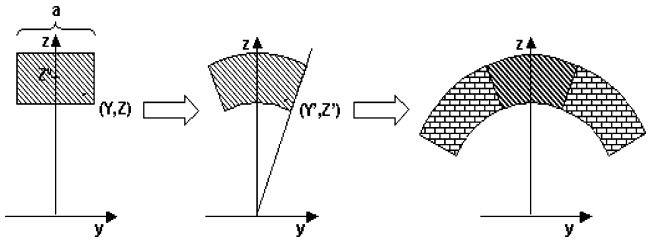

Figure 11. Scheme of the procedure used to investigate the stability of the structure as a function of its curvature.

plane onto a section of an annulus, as shown in the first step of the scheme of Figure 11. The mapping is defined as

$$Y' = Z \sin\alpha Y$$

$$Z' = Z \cos\alpha Y$$

where $\alpha = 1/Z^0$. In this procedure the radius of curvature is $R = Z^0$.

We apply the following algorithm for determining whether the curved structure is more stable than the planar one. First, we bend the structure according to the above rule with a given radius of curvature, then replicate it twice, and rotate each replica around the curvature axis to the left and right side of the original, as shown in the second step of Figure 11. Next, the rotated replicas are kept fixed while the central part is optimized. Then, the optimized central part is replicated again and the procedure is repeated iteratively until the energy of the optimized structure converges.

We have applied the procedure for several different radii of curvature, and around each of the two periodic directions, *x* and *y*, of the planar elementary cell. A plot of the energy of the optimized curved structures, relative to that of the structure without curvature, as a function of curvature, defined as $1/R$, together with an example of one such structure, are shown in Figure 12. From this plot it is clear that the structure would be stabilized by a curvature around the *x* axis, as expected based on the voids seen along the *y* axis shown in Figure 8. Analogous *y*-axis curvature does not lead to statistically significant stabilization. This leads to the conclusion that a cylindrical configuration would be the most stable one for the self-assembled system considered here. Such a configuration would not only retain the favorable antiparallel orientation of the dipoles and the hydrogen bonds along the axis of the cylinder, it would also stabilize the micelle by the increased hydrophobic attraction between the tails. It should be pointed out that the approach presented here can only provide an indication about the direction of curvature. The obtained radius of curvature is a lot larger than the experimental one, which is approximately equal to the length of the amphiphile (4 nm). We expect that it should be possible to reproduce the experimental radius of curvature with a more rigorous approach in which the dynamics of a whole elementary "slice" of the cylinder is studied, rather than a fraction of it. Unfortunately, such studies are currently computationally unfeasible, due to the large size of the system. Despite this, we believe that the approach described here is reliable for qualitative predictions of the curvature of similar self-assembled nanostructures.

6. Conclusions

We have presented a novel approach to study self-assembly processes based on all-atom empirical force field calculations, and have applied it to zwitterionic peptide amphiphiles forming cylindrical micelles intended for applications in new medical treatments. We have optimized the diad of the amphiphiles by statistical sampling of the full range of initial conditions for the mutual orientation of two amphiphiles, after which the most stable diad is selected and used as an elementary starting unit for building the self-assembly. Quartets are formed from the optimized diad by similar sampling of the possible initial conditions for the mutual orientation of two diads, and are then

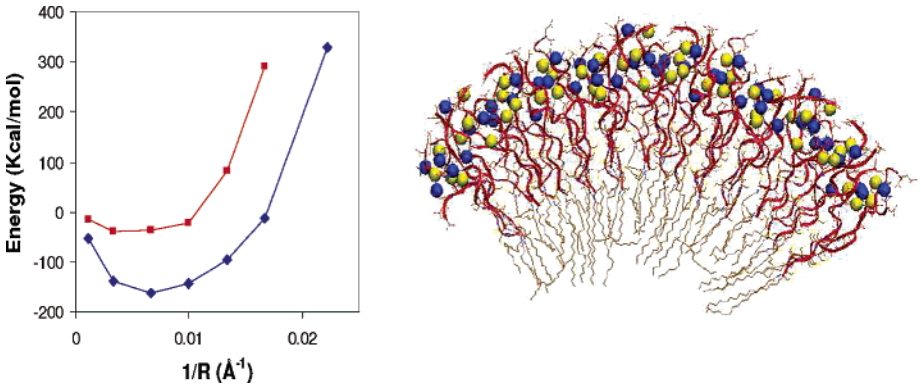

Figure 12. Left panel shows the energy of the optimized structure, relative to that of the structure without curvature, as a function of the curvature $1/R$ around the *x* (blue) and *y* (red) directions. The minimum in the *x* curve indicates that the structure would curve around that axis. The right panel shows the optimized curved structure around the *x* direction for $R = 60$ Å.

used to form 4×4 supercells to be optimized in PBC. Implicit solvent is applied to these systems, and the most stable structure is selected for further studies. It is subjected to MD simulations with explicit water solvent. The results of these simulations reveal an interesting picture of the structure of the assembly. In the upper parts of the hydrophilic headgroups the dipoles of the amphiphiles are oriented in an antiparallel fashion along the cylinder axis; in the lower, rigid part of the headgroups hydrogen bonds form a parallel beta sheet with the same orientation as the dipoles. These results are compatible with the available experimental data[14−17] and provide structural details of the assembly that the experiments cannot give. A comparison with our previous work[13] shows that using explicit solvent in the simulations leads to stronger screening of the electrostatic interactions in the hydrophilic headgroups compared to the implicit solvent models, which has been attributed to the penetration of the water molecules inside the headgroups and the formation of hydrogen bonds between them and the peptides. However, the relative orientation of the dipoles and hydrogen bonds within the micelle is retained. We have also found out that the structure is very stable on the time scale of the simulation.

The method used in this work employs a shortcut procedure for finding the thermodynamically most stable structure based on a hierarchical "assembly" of subunits. This procedure makes the approach computationally feasible, albeit less rigorous than the standard Monte Carlo or molecular dynamics simulation methods. However, the lack of rigor is compensated by the sampling of a very large number of initial conditions at each stage of the "assembly" to ensure that the most stable final structure is obtained. Therefore, we expect that this method should be applicable to a wide range of similar self-assembling systems, and it should be possible to use it to predict and study the structure and properties of many new materials based on them. This approach is capable of predicting not only the overall shape of such assemblies, but also their atomistically detailed structure, which is beyond the capability of modern experiments and can be very useful when planning the synthesis of a new material with specific desired characteristics, such as possession of certain biologically active functional groups for applications in medicine and biotechnology.

Acknowledgment. S.T. is thankful to J. Hartgerink and S. Stupp for valuable discussions. We are grateful to the DoD/MURI program for support of this research.

References and Notes

(1) Leininger, S.; Olenyuk, B.; Stang, P. J. *Chem. Rev.* **2000**, *100*, 853.
(2) Redl, F. X.; Cho, K. S.; Murray, C. B.; O'Brien, S. *Nature* **2003**, *423*, 968.
(3) Reches M.; Gazit, E. *Science* **2003**, *300*, 625.
(4) Yan, H.; Park, S. H.; Finkelstein, G.; Reif, J. H.; LaBean, T. H. *Science* **2003**, *301*, 1882.
(5) Sellmyer, D. J. *Nature* **2002**, *420*, 374.
(6) Joannopoulos, J. D. *Nature* **2001**, *414*, 257.
(7) Lehn, J. M. *Supramolecular Chemistry: Concepts and Perspectives*; VCH: Weinheim, Germany, 1995.
(8) Atwood, J. L.; Lehn, J. M.; Davis, J. E. D.; MacNicol, D. D.; Vogtle, F. *Comprehensive Supramolecular Chemistry*; Pergamon: New York, 1996.
(9) Kenward M.; Whitmore, M. D. *J. Chem. Phys.* **2002**, *116*, 3455.
(10) Lopez, C. F.; Moore, P. B.; Shelley, J. C.; Shelley, M. Y.; Klein, M. L. *Comput. Phys. Commun.* **2002**, *147*, 1.
(11) Tsonchev, S.; Schatz, G. C.; Ratner, M. A. *Nano Lett.* **2003**, *3*, 623.
(12) Tsonchev, S.; Schatz, G. C.; Ratner, M. A. *J. Phys. Chem. B* **2004**, *108*, 8817.
(13) Tsonchev, S.; Troisi, A.; Schatz, G. C.; Ratner, M. A. *Nano Lett.* **2004**, *4*, 427.
(14) Hartgerink, J. D.; Beniash, E.; Stupp, S. I. *Science* **2001**, *294*, 1684.
(15) Hartgerink, J. D.; Beniash, E.; Stupp, S. I. *Proc. Natl. Acad. Sci. U.S.A.* **2002**, *99*, 5133.
(16) Niece, K. L.; Hartgerink, J. D.; Donners, J. J. J. M.; Stupp, S. I. *J. Am. Chem. Soc.* **2003**, *125*, 7146.
(17) Silva, G. A.; Czeisler, C.; Niece, K. L.; Beniash, E.; Harrington, D. A.; Kessler, J. A.; Stupp, S. I. *Science* **2004**, *303*, 1352.
(18) Allinger, N. L.; Yuh, Y. H.; Lii, J.-H. *J. Am. Chem. Soc.* **1989**, *111*, 8551. Lii J.-H.; Allinger, N. L. *J. Comput. Chem.* **1998**, *19*, 1001.
(19) Ponder J. W.; Richards, F. M. *J. Comput. Chem.* **1987**, *8*, 1016. Kundrot, C. E.; Ponder, J. W.; Richards, F. M. *J. Comput. Chem.* **1991**, *12*, 402. Dudek M. J.; Ponder, J. W. *J. Comput. Chem.* **1995**, *6*, 791.
(20) Andersen, H. C. *J. Comput. Phys.* **1983**, *52*, 24.
(21) Berendsen, H. J. C.; Postma, J. P. M.; van Gunsteren, W. F.; DiNola A.; Haak, J. R. *J. Chem. Phys.* **1984**, *81*, 3684.
(22) Eisenberg D.; McLachlan, A. D. *Nature* **1986**, *319*, 199.
(23) Ooi, T.; Oobatake, M.; Nemethy, G.; Scheraga, H. A. *Proc. Natl. Acad. Sci. U.S.A.* **1987**, *84*, 3086.
(24) Hawkins, G. D.; Cramer, C. J.; Truhlar, D. G. *Chem. Phys. Lett.* **1995**, *246*, 122.
(25) Humphrey, W.; Dalke, A.; Schulten, K. *J. Mol. Graphics* **1996**, *14.1*, 33.
(26) A similar histogram of the distribution of the intermolecular hydrogen bonds between the upper, flexible parts of the headgroups reveals their random orientations and lack of preferential direction.